A Journal of the Gesellschaft Deutscher Chemiker

Angewandte International Edition GDCh Chemie

www.angewandte.org

Accepted Article

Title: Structural Evolution of Giant Polyoxometalate: From "Keplerate" to "Lantern" Type Mo132 for Improved Oxidation Catalysis

Authors: Jiang Liu, Nan Jiang, Jiao-Min Lin, Zhi-Bin Mei, Long-Zhang Dong, Yi Kuang, Jing-Jing Liu, Su-Juan Yao, Shun-Li Li, and Ya-Qian Lan

To be cited as: *Angew. Chem. Int. Ed.* **2023**, e202304728

Link to VoR: https://doi.org/10.1002/anie.202304728

WILEY VCH

10.1002/anie.202304728

WILEY-VCH

RESEARCH ARTICLE

Structural Evolution of Giant Polyoxometalate: From "Keplerate" to "Lantern" Type Mo_{132} for Improved Oxidation Catalysis

Jiang Liu,[†[a]] Nan Jiang,[†[a]] Jiao-Min Lin*[a], Zhi-Bin Mei,[a] Long-Zhang Dong,[a] Yi Kuang,[a] Jing-Jing Liu,[a] Su-Juan Yao,[a] Shun-Li Li[a] and Ya-Qian Lan*[a]

[a] Prof. J. Liu, N. Jiang, Prof. J.-M. Lin, Z.-B. Mei, Dr. L.-Z. Dong, Y. Kuang, J.-J. Liu, S.-J. Yao, Prof. S.-L. Li and Prof. Y.-Q. Lan
School of Chemistry, National and Local Joint Engineering Research Center of MPTES in High Energy and Safety LIBs, Engineering Research Center of MTEES (Ministry of Education), and Key Lab. of ETESPG (GHEI).
South China Normal University
Guangzhou, 510006, P. R. China.
E-mail: linjm@m.scnu.edu.cn; yqlan@m.scnu.edu.cn
[†] These authors contributed equally to this work.

Supporting information for this article is given via a link at the end of the document.((Please delete this text if not appropriate))

Abstract: Structural variants of high-nuclearity clusters are extremely important for their modular assembly study and functional expansion, yet the synthesis of such giant structural variants remains a great challenge. Herein, we prepared a lantern-type giant polymolybdate cluster (***L*-Mo$_{132}$**) containing equal metal nuclearity with the famous Keplerate type Mo_{132} (***K*-Mo$_{132}$**). The skeleton of ***L*-Mo$_{132}$** features a rare truncated rhombic triacontrahedron, which is totally different with the truncated icosahedral ***K*-Mo$_{132}$**. To the best of our knowledge, this is the first time to observe such structural variants in high-nuclearity cluster built up of more than 100 metal atoms. Scanning transmission electron microscopy reveals that ***L*-Mo$_{132}$** has good stability. More importantly, because the pentagonal $[Mo_6O_{27}]^{n-}$ building blocks in ***L*-Mo$_{132}$** are concave instead of convex in the outer face, it contains multiple terminal coordinated water molecules on its outer surface, which make it expose more active metal sites to display superior phenol oxidation performance, which is more higher than that of ***K*-Mo$_{132}$** coordinated in M=O bonds on the outer surface.

Introduction

Polyoxometalates (POMs) are a class of discrete inorganic clusters built up by early transition metal-oxo (e.g. W, Mo and V) units.[1] POMs have a wide variety of structures and physicochemical properties,[2] which render them great potential for application in the areas of catalysis,[3] medicine,[4] material design[5] and solid-state devices.[6] For POMs, their structures are mainly dependent on the number and the combinatorial/connected mode of the metal-oxo units. Thus, in addition to the formation of a large number of structures with metal nuclearities rang from several to hundreds or even more,[7] the self-assembly of metal-oxo units can also able to construct POM structural variants that contain the same metal numbers yet show quite different structures.[8] For example, the well-known Keggin $\{PMo_{12}O_{40}\}^{n-}$ has α, β, γ, δ, and ε structural variants resulting from the different connected modes of the $\{Mo_3O_{13}\}$ units.[9] Moreover, these structural variants can show some different physical and chemical properties, such as light absorption, redox and catalytic activities.[2, 10] In this context, the construction of POM structural variants that contain the same metal nuclearity while show large structural differences are significant since they can not only enrich the structures and properties of POM chemistry, but also provide a unique platform for the comparative study of the structural assembly and the structure-property relationships. Nevertheless, owing to the synthetic challenge, the know examples of POM structural variants are still relatively few.[11] In particular, high nuclearity POM structural variants (e.g. metal nuclearity > 100), to the best of our knowledge, have not been reported thus far, which probably because of their more complex structural assembly.

Giant POMs, which usually possess high metal nuclearity and biomacromolecule-like size, have attracted tremendous attention in the past few decades.[7a, 12] The structures of giant POMs can be considered as the order and precise assembly of a range of metal-oxo building blocks (BBs), which appear structurally to be fundamental to this class of compounds. Because more metal-oxo BBs are involved into the self-assembly, the synthesis of giant POMs is usually more challenging. Over the past two decades, great efforts have been devoted to this field, and many ingratiating giant POMs, especially polymolybdate clusters, such as wheel-shaped Mo_{154} and $Mo_{100}Ce_6$,[13] Keplerate type Mo_{132} (denoted as ***K*-Mo$_{132}$**),[14] and lemon-shaped Mo_{368}[7f] have been synthesized by chemists. Generally, giant polymolybdate clusters contain reduced Mo centers, and thus conventional synthesis is usually carried out at room temperature as it was thought that the reduced Mo centers would be oxidized at high temperature. Recently, we and others found that elevated temperature can produce highly reduced polymolybdate clusters with unique structure types.[15] For example, we prepared a 240-nuclearity giant polymolybdate Mo_{240} with a regular pentagonal dodecahedral geometry via hydrothermal synthesis.[15a] This polymolybdate cage features high molybdenum reduction degree (proportion of Mo^{5+} is 0.75) and shows good stability in aqueous solution. We believe that it may provide more opportunities to explore more new giant POMs with the change of the hydrothermal reaction conditions.

Herein, we report a new giant reduced polymolybdate clusters $Na_3(NH_4)_9H_{24}[H_{30}Mo^{VI}_{92}Mo^{V}_{10}Mo^{IV}_{30}(H_2O)_{36}O_{382.4}S_{9.6}(SO_4)_2]\cdot ca.150H_2O$ (= $Na_3(NH_4)_9H_{24}$***L*-Mo$_{132}$**$\cdot ca.150H_2O$) with a Chinese-lantern like appearance via hydrothermal synthesis. Structural analysis revealed that the skeleton of ***L*-Mo$_{132}$** is built up by 12 pentagonal $[Mo_6O_{27}]^{n-}$ BBs, 10 triangular $[Mo_3O_{12}S]^{n-}$ BBs

10.1002/anie.202304728
WILEY-VCH

RESEARCH ARTICLE

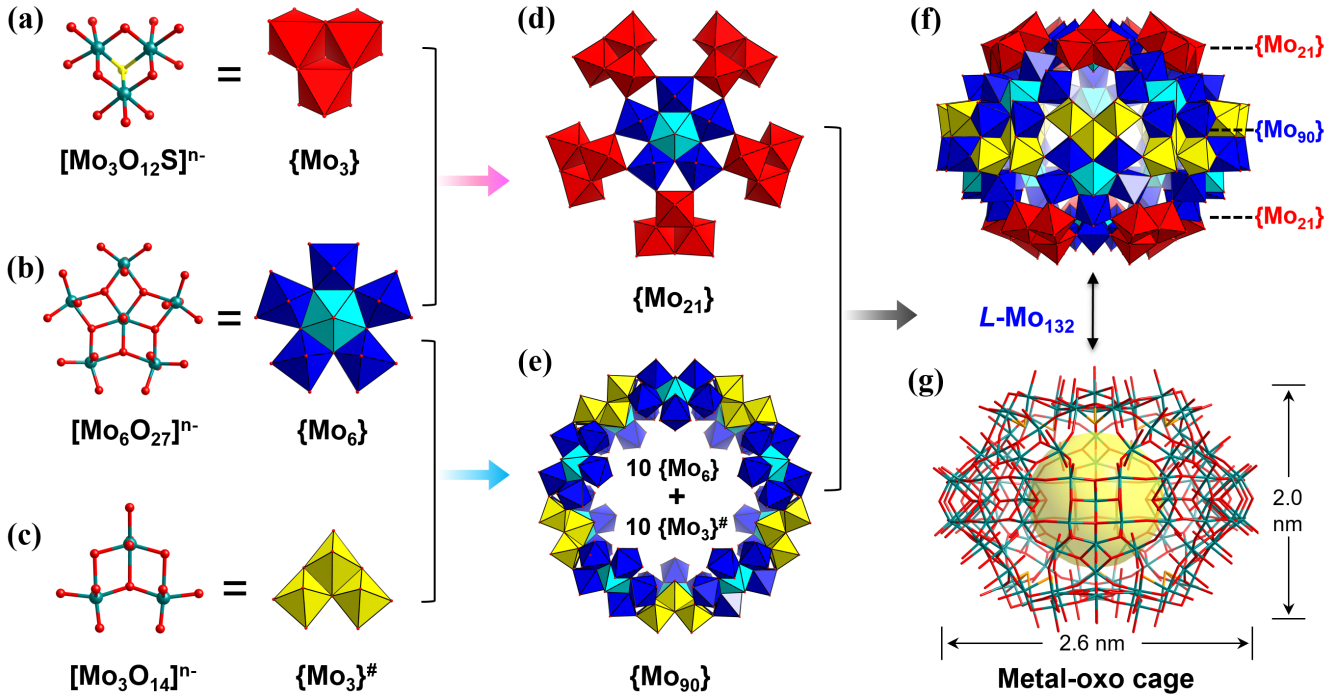

Figure 1. Crystal structure of ***L*-Mo$_{132}$**. Ball-and-stick and polyhedron views of the (a) {Mo$_3$}, (b) {Mo$_6$} and (c) {Mo$_3$}$^{\#}$ building blocks. Color code: teal ball, Mo; red ball, O; yellow ball, S. Polyhedral views of the (d) {Mo$_{21}$} and (e) {Mo$_{90}$} units. (f) Side view of ***L*-Mo$_{132}$** in polyhedral representation. (g) Ball-and-stick view of the structure of ***L*-Mo$_{132}$**.

and 10 ^-shaped [Mo$_3$O$_{14}$]$^{n-}$ BBs, featuring a rare distorted truncated rhombic triacontrahedron. Interesting, ***L*-Mo$_{132}$** contains the same numbers of Mo atoms with the famous Keplerate type Mo$_{132}$ (***K*-Mo$_{132}$**, truncated icosahedron), while displays a new type of structure. ***L*-Mo$_{132}$** exhibits good structural stability and can be visualized by scanning transmission electron microscopy (STEM) imaging. Moreover, because the pentagonal [Mo$_6$O$_{27}$]$^{n-}$ BBs in ***L*-Mo$_{132}$** are concave in the outer face, it contains multiple terminal coordinated H$_2$O molecules on the outer surface, which offers great potential for creating multiple Mo-metal activate sites for catalysis. Thus, we investigated its catalytic performance in the phenol oxidative reactions with tert-butyl hydroperoxide (TBHP) as oxidant. The results revealed that ***L*-Mo$_{132}$** can serve as an effective homogeneous catalyst for activating TBHP to oxidize phenol derivatives to form corresponding *p*-benzoquinones with high conversion and selectivity. In contrast, ***K*-Mo$_{132}$** and Keggin H$_3$[PMo$_{12}$O$_{40}$], whose terminal oxygen atoms at the outer surface are mainly strongly coordinated deprotonated oxygen atoms, show low catalytic activity under similar reaction conditions. This work not only constructs an interesting giant polymolybdate cluster, but also shows that POMs with terminal coordinated H$_2$O molecules on their outer surface may be more easily to release the catalytic activity of the metal centers than that with strongly coordinated deprotonated oxygen atoms.

Results and Discussion

***L*-Mo$_{132}$** was synthesized via reaction of an aqueous mixture of (NH$_4$)$_6$Mo$_7$O$_{24}$·4H$_2$O, N$_2$H$_4$·2HCl, Na$_2$S$_2$O$_4$ and a small amount of H$_2$SO$_4$ in a small capped vial at 120 °C for 3 days (Figure S1). The (NH$_4$)$_6$Mo$_7$O$_{24}$·4H$_2$O can be replaced by Na$_2$MoO$_4$ when a small amount of diluted HCl or HBr was added to keep the pH around 1.0. In this reaction, in addition to the accurate pH tuning that is generally required for the synthesis of reduced polymolybdate clusters, the coexisting of Na$_2$S$_2$O$_4$ and N$_2$H$_4$·2HCl as reducing agents and the constant high temperature (hydrothermal reaction) are also found to be important variables. The Na$_2$S$_2$O$_4$ not only serves as a reducing agent, but also provides S^{2-} anion in situ for the formation of the S-contained trinuclear [Mo$_3$O$_{12}$S]$^{n-}$ BBs in ***L*-Mo$_{132}$**. Without Na$_2$S$_2$O$_4$, only a small amount of dark red polygonal crystals that determined to be our previous reported Mo$_{240}$ was obtained (Figure S1). On the other hand, the constant high temperature and the present of N$_2$H$_4$·2HCl reductant may promote the reduction of Mo^{VI} to Mo^{IV} and Mo^{V}, and the formation of this reduced polymolybdate cluster.

Single-crystal X-ray diffraction (XRD) analysis reveals that ***L*-Mo$_{132}$** crystallizes in the monoclinic space group *C*2/*m* (Table S1, Figure S2)[16]. The structure of ***L*-Mo$_{132}$** is compose of 12 pentagonal [Mo$_6$O$_{27}$]$^{n-}$ (denoted as {Mo$_6$}) BBs, 10 S-contained trinuclear [Mo$_3$O$_{12}$S]$^{n-}$ (denoted as {Mo$_3$}) BBs and 10 trinuclear BBs [Mo$_3$O$_{14}$]$^{n-}$(denoted as {Mo$_3$}$^{\#}$) (Figure 1). The S-contained {Mo$_3$} BB is built up by three {MoO$_5$S} octahedras through sharing three edges and a common μ_3-S vertex (Figure 1a), showing a regular triangle configuration with C_{3v} symmetry. The core structure this {Mo$_3$} BB is similar with that of the Na$_2$[Mo$_3$(μ_3-S)(μ_2-O)$_3$(glyc)$_3$(2-mim)$_3$]·1.5H$_2$O (Figure S1)[17], which reported recently by Zhou, but has not been used as BBs for the construction of giant POMs by far.

10.1002/anie.202304728

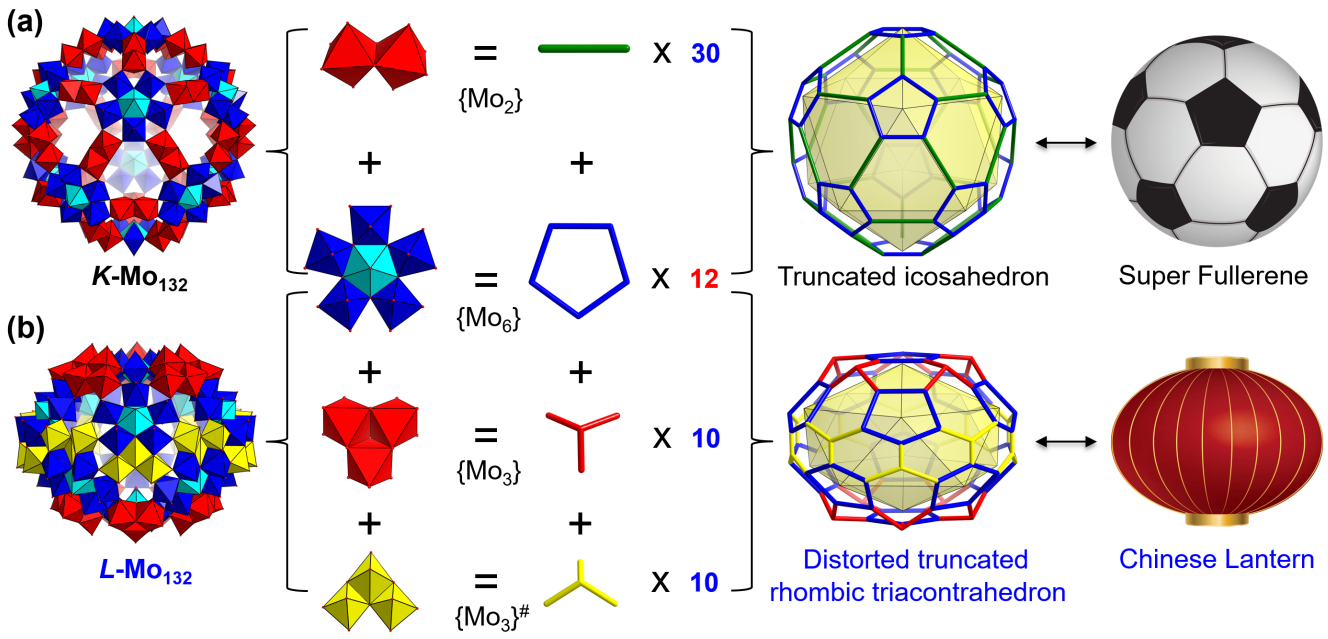

Figure 2. Simplify of the structures of (a) ***K*-Mo$_{132}$** as a truncated icosahedron and (b) ***L*-Mo$_{132}$** as a distorted truncated rhombic triacontrahedron by considering the pentagonal {Mo$_6$} BB as a 5-connected face, the {Mo$_2$} BB as a 2-connected linker, and the {Mo$_3$} and {Mo$_3$}$^{\#}$ BBs as 3-connected linker, respectively. In the truncated icosahedron and the distorted truncated rhombic triacontrahedron, the 12 pentagonal faces locate on the vertexes of the yellow icosahedron. The appearance of ***K*-Mo$_{132}$** is like a super fullerene and that of ***L*-Mo$_{132}$** is like a Chinese lantern.

Five {Mo$_3$} BBs connect with one pentagonal {Mo$_6$} BB through ten μ_2-O atoms to build a cap-like {Mo$_{21}$} unit with C_{5V} symmetry (Figure 1b, d). In this {Mo$_{21}$} unit, the pentagonal {Mo$_6$} BB and the triangle {Mo$_3$} BB connect together either in a vertex-to-edge mode or in a vertex-to-vertex mode (Figure S3), resulting crystallographic disorder of the {Mo$_3$} BBs. Structure free refinement results revealed that the vertex-to-edge mode has occupancy of about 90%, indicating that it is the primary connected mode in this structure.

In addition to the {Mo$_3$} BB, there is another type of trinuclear BB, {Mo$_3$}$^{\#}$, in ***L*-Mo$_{132}$**. Each {Mo$_3$}$^{\#}$ BB is formed by three {MoO$_6$} octahedras through sharing two edges (Figure 1c), showing a ^-shaped configuration with C_{2V} symmetry. This {Mo$_3$} BB also serves as 3-connected linker to connect with two pentagonal {Mo$_6$} BBs through four μ_2-O atoms, and another one pentagonal {Mo$_6$} BB through sharing four edges, resulting in a wheel shaped {Mo$_{90}$} unit with D_{5d} symmetry containing ten {Mo$_3$} and ten {Mo$_6$} BBs (Figure 1e). This wheel shaped {Mo$_{90}$} unit can also be viewed as an assembly of ten {Mo$_8$} BBs (compose of one pentagonal {Mo$_6$} BB and two {Mo$_1$} units) and ten {Mo$_1$} units, as illustrated in many classic giant Molybdenum Blue wheels, such as Mo$_{154}$, Mo$_{100}$Ce$_6$ and Mo$_{90}$Ce$_{10}$.[13b, 18]

The wheel shaped {Mo$_{90}$} unit was further capped by two {Mo$_{21}$} units from top side and down side, resulting the ***L*-Mo$_{132}$** with a hollow structure (Figure 1f, Figure S5). In ***L*-Mo$_{132}$**, the wheel shaped {Mo$_{90}$} unit and two {Mo$_{21}$} units connect together by the 5-connected pentagonal {Mo$_6$} BBs from the {Mo$_{90}$} unit and the 3-connected {Mo$_3$} BBs from the {Mo$_{21}$} unit (owing to the disorder of {Mo$_3$} BBs, the connection between the {Mo$_6$} and {Mo$_3$} BBs also in vertex-to-edge mode or vertex-to-vertex mode, Figure S4). It is interesting that such unique assembly mode (one wheel + two caps), associating with the hollow structure, makes the appearance of ***L*-Mo$_{132}$** look quite like a Chinese lantern (Figure 1f, 2b). The dimensions of this lantern type ***L*-Mo$_{132}$** are about 2.6 × 2.6 × 2.0 nm (Figure 1g and Figure S6), and that of its inner cavity are approximating 1.40 × 1.40 × 1.06 nm (van der Waals radii of atoms considered). These parameters are comparable to those of the ball-shaped Mo$_{72}$M$_{30}$ (M = Fe, V),[19] but small than those of ***K*-Mo$_{132}$** and our recently reported Mo$_{240}$.[14,15a]

To make a better comparison between ***L*-Mo$_{132}$** and the classic Keplerate type ***K*-Mo$_{132}$** that composed of 12 pentagonal {Mo$_6$} BBs and 30 edge-shared {Mo$_2$} BBs, we have simplified these two structures by considering the pentagonal {Mo$_6$} BB as a 5-connected face, the {Mo$_3$} and {Mo$_3$}$^{\#}$ BBs as 3-connected linker, and the {Mo$_2$} BB as a 2-connected linker(Figure 2), respectively. As shown in Figure 2, ***L*-Mo$_{132}$** can be simplified as a distorted truncated rhombic triacontrahedron containing 12 pentagonal and 30 hexagonal faces, while ***K*-Mo$_{132}$** can be simplified as a truncated icosahedron with 12 pentagonal and 20 hexagonal faces. Owing to the irregular 3-connected linkers of the {Mo$_3$}$^{\#}$ BBs, the structure of ***L*-Mo$_{132}$** is not the regular truncated rhombic triacontrahedron (Figure 2b). It is worth noting that the pentagonal {Mo$_6$} BBs in ***L*-Mo$_{132}$** are concave instead of convex in the outer face, which is different from that in ***K*-Mo$_{132}$**, and gives ***L*-Mo$_{132}$** the lantern-shape. On the other hand, although both ***L*-Mo$_{132}$** and ***K*-Mo$_{132}$** contain the same numbers of the pentagonal {Mo$_6$} BBs, the shorter size but higher connected numbers of the {Mo$_3$} and {Mo$_3$}$^{\#}$ linkers in ***L*-Mo$_{132}$** make it show smaller in size and more complex in polyhedral geometry, as compared with that of ***K*-Mo$_{132}$**. It is worth noting that the know examples of molecules/clusters with truncated rhombic triacontrahedral structures are still quite few, with representative examples such

as fullerene C_{80} and recently reported two inorganic-organic hybrid cages MOP-3 and MOP-4.[20] To our knowledge, ***L*-Mo$_{132}$** is the first giant inorganic hollow truncated rhombic triacontrahedral cluster synthesized by far.

Based on the same numbers of Mo atoms and the significant structural difference, ***L*-Mo$_{132}$** and ***K*-Mo$_{132}$** can be regarded as a couple of structural variants, which is rare observed among giant POMs. Bond valence sum analysis (BVS) and redox titration indicate that there are about 92 Mo^{VI}, 10 Mo^{V} and 30 Mo^{IV} centers (mainly from the {Mo_3} BBs) in ***L*-Mo$_{132}$** (Table S2), which is slightly different from that of ***K*-Mo$_{132}$** (72 Mo^{VI} and 60 Mo^{V} centers) (Table S3). The 30 Mo^{IV} atoms are from the 10 {Mo_3} BBs, and the 10 Mo^{V} atoms are localized at the backbone of the {Mo_{90}} ring, which are consistent with previous reported works.[15b, 17] The multiple Mo^{IV} and Mo^{V} centers in ***L*-Mo$_{132}$** suggest that it also belongs to reduced polymolybdate cluster. For the O atoms, although the Mo centers in ***L*-Mo$_{132}$** and ***K*-Mo$_{132}$** adopting the same coordinated modes (12 seven-coordinated Mo centers and 120 six-coordinated Mo centers), the total numbers of the O atoms in the skeleton of ***L*-Mo$_{132}$** (424 O atoms) is lesser than that of ***K*-Mo$_{132}$** (504 O atoms) (Table S3). This because more O atoms in ***L*-Mo$_{132}$** are served as bridged O atoms (164 μ_2-O, 76 μ_3-O and 10 μ_4-O), as compared with that of ***K*-Mo$_{132}$** (180 μ_2-O and 60 μ_3-O) (Table S3). Besides, ***L*-Mo$_{132}$** contains 10 μ_3-S atoms. These bridged O and S atoms in ***L*-Mo$_{132}$** may increase its stability. Bond length analysis and BVS reveals 30 singly and 36 doubly protonated oxygen atoms (coordination water) in ***L*-Mo$_{132}$**. Most of the coordination water located on the outer surface of ***L*-Mo$_{132}$** (Figure S7), which is different from that of ***K*-Mo$_{132}$**, whose coordination water mainly localised in its inner surface (Figure S8). This is main because the pentagonal {Mo_6} BBs of ***L*-Mo$_{132}$** are concave in the outer face, while that in ***K*-Mo$_{132}$** are convex in the outer face. The coordination water on the outer surface of ***L*-Mo$_{132}$** may offer great potential for creating multiple opening Mo-metal activate sites for catalysis.

The phase purity of the as-synthesized ***L*-Mo$_{132}$** sample was confirmed by power XRD (Figure 3a). Thermogravimetric analysis (TGA) revealed that ***L*-Mo$_{132}$** exhibits a sharp weight loss of 11.5% occurring between 25 and 120 ºC, corresponding to the loss of about 150 free water molecules, and then a gradual weight of 3.9% from 120 to 200 ºC is attributed to the removal of the coordinated water molecules and the counter cations (Figure S9). The Fourier transformed infrared (FT-IR) spectrum of the as-synthesized ***L*-Mo$_{132}$** displays strong peaks at 967 and 907 cm^{-1}, corresponding to the stretching vibrations of the terminal Mo=O and Mo–O bonds, respectively (Figure S10).[19] The bands at 645, 574 and 523 cm^{-1} should be attributed to vibrations of the Mo–O–Mo bridges. The Mo 3d X-ray photoelectron spectroscopy (XPS) spectrum of the as-synthesized ***L*-Mo$_{132}$** shows six peaks at 236.1, 235.0, 234.4, 232.9, 231.7 and 230.9 eV, corresponding to the binding energies of Mo^{VI}-$3d_{3/2}$, Mo^{V}-$3d_{3/2}$, Mo^{IV}-$3d_{3/2}$, Mo^{VI}-$3d_{5/2}$, Mo^{V}-$3d_{5/2}$ and Mo^{IV}-$3d_{5/2}$, respectively (Figure 3b).[21] This suggests the Mo^{VI}, Mo^{V} and Mo^{IV} species in ***L*-Mo$_{132}$**. In the S 2p XPS spectrum, two peaks at 162.7 and 169.1 eV were observed, which could be assigned to S^{2-} in the {Mo_3} BB and the S^{6+} in the terminal coordinated SO_4^{2-}, respectively (Figure S11).[21] The UV-vis-NIR spectrum of ***L*-Mo$_{132}$** exhibits absorption band around 708 nm (Figure S12), which is slightly different with that of the classic molybdenum blue clusters (with absorption peak at 745 nm). This fact is probably attributed to further intervalence charge transfers resulted from the Mo^{IV} species in ***L*-Mo$_{132}$**.

The stability of ***L*-Mo$_{132}$** was characterized by STEM, FT-IR and UV-vis spectra. To prepare a sample for STEM imaging, we synthesized a tetrabutylammonium (TBA) salt of ***L*-Mo$_{132}$** (denoted as ***L*-Mo$_{132}$-TBA**) via the reaction of ***L*-Mo$_{132}$** with TBA·Br in H_2O. The obtained ***L*-Mo$_{132}$-TBA** shows good solubility in acetonitrile, which makes it easily to prepare monodispersed cluster/particle of ***L*-Mo$_{132}$** on a silicon chip for STEM imaging. As shown in Figure 3d and Figure S13, identifiable bright dots with uniform size distribution of 1.8 (±2) × 2.4 (±2) nm could be observed in the dark-field STEM image. Besides, the size of the bright dots is well consistent with the core size of ***L*-Mo$_{132}$** determined by X-ray crystallography, indicating the structure of ***L*-Mo$_{132}$** was maintained during the preparation of ***L*-Mo$_{132}$-TBA**. In addition, in the STEM image, it is interesting to observe that many of the ***L*-Mo$_{132}$** particles form linear aggregates, which is quite consistent with the face-to-face (the face of the cap) molecular packing of ***L*-Mo$_{132}$** (Figure 3e). We then determined the FT-IR and UV-vis spectra of ***L*-Mo$_{132}$-TBA**. As shown in Figure S10, the FT-IR spectra of ***L*-Mo$_{132}$-TBA** and its parent crystals the as-synthesized ***L*-Mo$_{132}$** display almost consistent absorption peaks. Moreover, the UV-vis spectra of ***L*-Mo$_{132}$-TBA** in acetonitrile solution and ***L*-Mo$_{132}$** in aqueous solution show consistent absorptions around 302 nm (Figure 3c). These results suggest that ***L*-Mo$_{132}$** should has good structural stability.

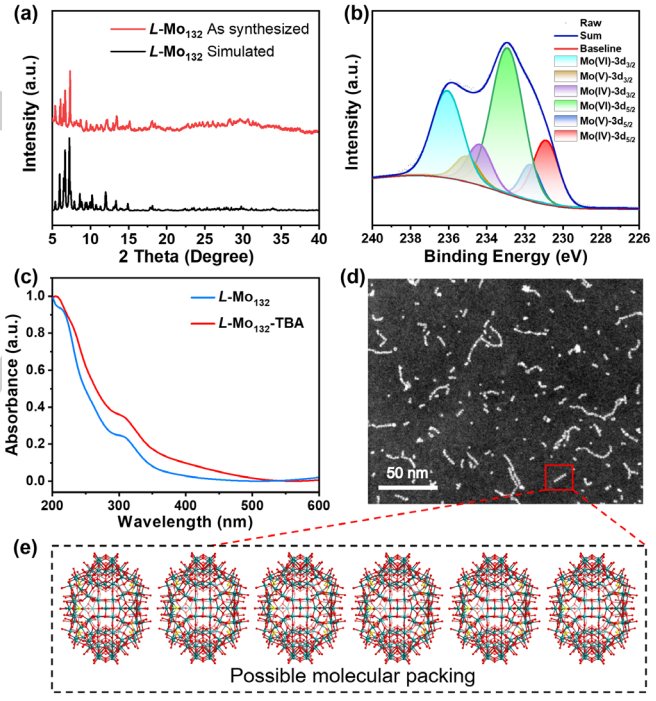

Figure 3. (a) Power XRD patterns of the as-synthesized ***L*-Mo$_{132}$**. (b) X-ray photoelectron spectrum of Mo in ***L*-Mo$_{132}$**. (c) UV-vis spectra of ***L*-Mo$_{132}$** and ***L*-Mo$_{132}$-TBA**. (d) Dark-field STEM image of the particles of ***L*-Mo$_{132}$-TBA**. (e) A proposed possible ***L*-Mo$_{132}$** molecular packing mode for the observed linear particle aggregates in the STEM image.

Considering the good stability and the multiple potential opening Mo-metal sites at the outer surface of ***L*-Mo$_{132}$**, we further investigated it (using ***L*-Mo$_{132}$** directly, not ***L*-Mo$_{132}$-TBA**) as homogeneous catalyst for the phenol oxidative reactions with tert-butyl hydroperoxide (TBHP) as oxidant. Selective oxidation of substituted phenols to corresponding *p*-benzoquinones (*p*-BQs) have attracted great research attention since *p*-BQs are key feedstocks for the synthesis of many high value fine chemicals

10.1002/anie.202304728

and biologically active compounds.[22] For this reaction, previous study revealed that the metal center of the catalyst usually involve in the activation of oxidant through forming temporary coordination bonds during the catalytic process.[23] Thus, we think that ***L*-Mo$_{132}$** with multiple potential opening Mo-metal sites at its outer surface may has good catalytic performance for this reaction.

Firstly, the oxidation of 2-tert-Butylphenol to 2-tert-Butyl-1,4-benzoquinone was selected as a model reaction and the optimized reaction conditions were screened (Table S4). The results revealed that ***L*-Mo$_{132}$** can serves as an effective homogeneous catalyst for activating TBHP to oxidize 2-tert-Butylphenol into 2-tert-Butyl-1,4-benzoquinone in acetonitrile at 80 °C. The conversion efficiency reaches 99% within 6 h under this reaction condition and the 2-tert-Butyl-1,4-benzoquinone selectivity is close 100% (Table 1, Figure S14-S16). In addition, control experiments revealed that the conversion efficiency of 2-tert-Butylphenol to 2-tert-Butyl-1,4-benzoquinone was greatly limited in the absence of ***L*-Mo$_{132}$** or oxidant TBHP under similar conditions (Table S4, Figure S17), suggesting ***L*-Mo$_{132}$** and TBHP are important catalyst and oxidant for this reaction, respectively.

Table 1. Catalytic oxidation of substituted phenols to corresponding *p*-benzoquinones [a]

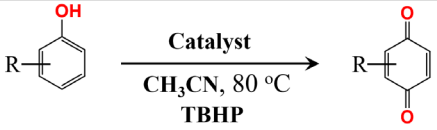

Entry	Catalyst	Substrate	Conv. (%)[d]	Sel. (%)[d]
1	***L*-Mo$_{132}$**		99	99
2	***K*-Mo$_{132}$**		44	79
3	$H_3[PMo_{12}O_{40}]$		9	52
4	–		2	60
5[b]	***L*-Mo$_{132}$**		99	98
6[c]	***L*-Mo$_{132}$**		97	71
7	***L*-Mo$_{132}$**		94	88
8	***L*-Mo$_{132}$**		89	71

[a] Reaction conditions: catalyst (5 mg), substrate (0.1 mmol), CH_3CN (2 mL), tert-butyl hydroperoxide (TBHP, 100 μL), 80 °C, 6h. [b] Reaction time 5 h. [c] Reaction time 2 h. [d] Determined by GC.

Based on the above results, we used other phenol derivatives, including 2,6-Di-tert-butylphenol, 2,3,6-Trimethylphenol, 2,5-Dimethylphenol and 2,6-Dimethylphenol as substrates to further investigate the catalytic performance of ***L*-Mo$_{132}$** for this oxidation reaction under similar reaction conditions (Figure S18-S29). As expected, these substituted phenol derivatives can also be effectively transformed into the corresponding *p*-BQs with relatively high conversion efficiency (89-99%) and selectivity (71-98%) within 6 h (Table 1). These results suggest that compound ***L*-Mo$_{132}$** can indeed serve as homogeneous catalyst for this TBHP-based phenol oxidation reaction. In addition, although compound ***L*-Mo$_{132}$** serves as homogeneous catalyst in this reaction, it can be recovered easily through forming **TBA** salt precipitate (denoted as ***L*-Mo$_{132}$-TBA-P**) with TBA·Br in H_2O. We further used this recovered ***L*-Mo$_{132}$-TBA-P** as homogeneous catalyst under similar reaction condition. The result revealed that it shows moderate catalytic performance (the conversion efficiency of 2-tert-Butylphenol to 2-tert-Butyl-1,4-benzoquinone is about 45%, and the selectivity remains 99%), which probably because of the present of the TBA molecules, since the ***L*-Mo$_{132}$-TBA** that prepared from the as-synthesized ***L*-Mo$_{132}$** also exhibit moderate catalytic performance under similar reaction condition (Table S5). The FT-IR and UV-vis spectra of ***L*-Mo$_{132}$-TBA-P** after catalytic reaction exhibit similar absorption peaks with that of ***L*-Mo$_{132}$-TBA** (Figure S30-S31), suggesting that the structural integrity of ***L*-Mo$_{132}$** can be maintained after the catalytic test.

As comparison, we also investigated the catalytic activities of ***K*-Mo$_{132}$** and Keggin $H_3[PMo_{12}O_{40}]$, whose terminal oxygen atoms at the outer surface are mainly strongly coordinated O^{2-} anions, for this phenol oxidation reaction under similar reaction condition. The ***K*-Mo$_{132}$** was prepared according to the reference (Figure S32-S33).[14] The results revealed that, for ***K*-Mo$_{132}$** and Keggin $H_3[PMo_{12}O_{40}]$, the 2-tert-Butylphenol to 2-tert-Butyl-1,4-benzoquinone conversion efficiency are 44% and 9% (Figure S34-S35), respectively, which are higher than that without catalyst, but much lower than that with ***L*-Mo$_{132}$** as catalyst (Table 1), suggesting that ***L*-Mo$_{132}$** with multiple terminal coordinated water molecules at its outer surface has higher catalytic activity. This probably because the terminal coordinated H_2O molecules are easily to be removed to build opening metal activate sites during the catalytic process.[23b] Thus, ***L*-Mo$_{132}$** can activate TBHP effectively to oxidize 2-tert-Butylphenol into 2-tert-Butyl-1,4-benzoquinone. In contrast, the terminal coordinated O^{2-} anions with high bonding energy are usually hard to be detached from the metal centers. Thus, ***K*-Mo$_{132}$** and Keggin $H_3[PMo_{12}O_{40}]$ exhibit lower catalytic activities than ***L*-Mo$_{132}$**. Note that, for ***K*-Mo$_{132}$**, its potential opening Mo-metal sites (coordinated by H_2O molecules) are located in its hydrophilic inner surface, for which the hydrophobic substrate molecules are harder to reach, as compared with that at the outer surface. Therefore, it is reasonable that the catalytic activities of these three compounds following the order of ***L*-Mo$_{132}$** > ***K*-Mo$_{132}$** > $H_3[PMo_{12}O_{40}]$ for this phenol oxidation reaction.

Conclusion

In summary, a new giant polymolybdate cluster ***L*-Mo$_{132}$** with a Chinese-lantern like appearance and equal Mo-metal nuclearity with the well-known Keplerate type ***K*-Mo$_{132}$** has been synthesized for the first time. ***L*-Mo$_{132}$** has been fully structurally characterized and its structural difference with ***K*-Mo$_{132}$** has been analyzed. For ***L*-Mo$_{132}$**, its 12 pentagonal {Mo_6} BBs are assembled together by 10 triangle shaped {Mo_3} BBs and 10 ∧-shaped {Mo_3} BBs, featuring a rare distorted truncated rhombic triacontrahedron; while for ***K*-Mo$_{132}$**, its 12 pentagonal {Mo_6} BBs are connected by 30 linear {Mo_2} BBs, exhibiting a truncated icosahedron. In addition, for ***L*-Mo$_{132}$**, its pentagonal {Mo_6} BBs are concave instead of convex in the outer face, which gives it the lantern-

shape and multiple coordinated H_2O molecules on the outer surface. ***L*-Mo$_{132}$** can be regard as a structural variant of ***K*-Mo$_{132}$** and it shows good stability. More importantly, the structure of ***L*-Mo$_{132}$** contains multiple potential opening Mo-metal activate sites on its outer surface. As a result, ***L*-Mo$_{132}$** as homogeneous catalyst exhibits much better catalytic performance for the phenol oxidative reaction (using tert-butyl hydroperoxide as oxidant) than ***K*-Mo$_{132}$** and Keggin $H_3[PMo_{12}O_{40}]$ (also as homogeneous catalysts), whose outer surfaces are lock of potential opening metal sites (coordinated by O^{2-} anions). This work may shed some light on the design, synthesis and the exploration of the metal catalytic activity of giant POMs.

Acknowledgements

This study was financially supported by the NSFC (Grants 22225109, 92061101 and 22071109) and Guangdong Basic and Applied Basic Research Foundation (No. 2023A1515030097), and the Excellent Youth Foundation of Jiangsu Natural Science Foundation (No. BK20211593).

Keywords: polyoxometalate • structural variants • phenol oxidation

[1] D.-L. Long, R. Tsunashima, L. Cronin, *Angew. Chem. Int. Ed.* **2010**, *49*, 1736-1758.

[2] N. I. Gumerova, A. Rompel, *Nat. Rev. Chem.* **2018**, *2*, 2397-3358.

[3] a) I. A. Weinstock, R. E. Schreiber, R. Neumann, *Chem. Rev.* **2018**, *118*, 2680-2717; b) S.-S. Wang, G.-Y. Yang, *Chem. Rev.* **2015**, *115*, 4893-4962; c) S. Amthor, S. Knoll, M. Heiland, L. Zedler, C. Li, D. Nauroozi, W. Tobaschus, A. K. Mengele, M. Anjass, U. S. Schubert, B. Dietzek-Ivansic, S. Rau, C. Streb, *Nat. Chem.* **2022**, *14*, 321-327; d) N. Li, J. Liu, B.-X. Dong, Y.-Q. Lan, *Angew. Chem. Int. Ed.* **2020**, *59*, 20779-20793; e) Z. Zhang, Y. Liu, H. Tian, X. Ma, Q. Yue, Z. Sun, Y. Lu, S. Liu, *ACS Nano* **2021**, *15*, 16581-16588; f) L. Ni, G. Yang, Y. Liu, Z. Wu, Z. Ma, C. Shen, Z. Lv, Q. Wang, X. Gong, J. Xie, G. Diao, Y. Wei, *ACS Nano* **2021**, *15*, 12222-12236.

[4] a) A. Bijelic, M. Aureliano, A. Rompel, *Angew. Chem. Int. Ed.* **2019**, *58*, 2980-2999; b) J.-C. Liu, J.-F. Wang, Q. Han, P. Shangguan, L.-L. Liu, L.-J. Chen, J.-W. Zhao, C. Streb, Y.-F. Song, *Angew. Chem. Int. Ed.* **2021**, *60*, 11153-11157.

[5] a) A. Misra, K. Kozma, C. Streb, M. Nyman, *Angew. Chem. Int. Ed.* **2020**, *59*, 596-612; b) Q. Lu, X. Wang, *Adv. Sci.* **2022**, *9*, 2104225; c) J.-X. Liu, X.-B. Zhang, Y.-L. Li, S.-L. Huang, G.-Y. Yang, *Coord. Chem. Rev.* **2020**, *414*, 213260; d) S. Khlifi, J. Marrot, M. Haouas, W. E. Shepard, C. Falaise, E. Cadot, *J. Am. Chem. Soc.* **2022**, *144*, 4469-4477.

[6] a) L. Chen, W.-L. Chen, X.-L. Wang, Y.-G. Li, Z.-M. Su, E.-B. Wang, *Chem. Soc. Rev.* **2019**, *48*, 260-284; b) S. Chai, F. Xu, R. Zhang, X. Wang, L. Zhai, X. Li, H.-J. Qian, L. Wu, H. Li, *J. Am. Chem. Soc.* **2021**, *143*, 21433-21442.

[7] a) J.-C. Liu, J.-W. Zhao, C. Streb, Y.-F. Song, *Coord. Chem. Rev.* **2022**, *471*, 214734; b) I. Colliard, J. C. Brown, D. B. Fast, A. K. Sockwell, A. E. Hixon, M. Nyman, *J. Am. Chem. Soc.* **2021**, *143*, 9612-9621; c) A. V. Virovets, E. Peresypkina, M. Scheer, *Chem. Rev.* **2021**, *121*, 14485-14554; d) S.-R. Li, H.-Y. Wang, H.-F. Su, H.-J. Chen, M.-H. Du, L.-S. Long, X.-J. Kong, L.-S. Zheng, *Small Methods* **2021**, *5*, 2000777; e) M. Zhu, S. Han, J. Liu, M. Tan, W. Wang, K. Suzuki, P. Yin, D. Xia, X. Fang, *Angew. Chem. Int. Ed.* **2022**, *61*, e202213910; f) A. Müller, E. Beckmann, H. Bögge, M. Schmidtmann, A. Dress, *Angew. Chem. Int. Ed.* **2002**, *41*, 1162-1167.

[8] H. Sartzi, H. N. Miras, L. Vilà-Nadal, D.-L. Long, L. Cronin, *Angew. Chem. Int. Ed.* **2015**, *54*, 15488-15492.

[9] a) A. Müller, C. Beugholt, P. Kögerler, H. Bögge, S. Bud'ko, M. Luban, *Inorg. Chem.* **2000**, *39*, 5176-5177; b) P. Mialane, A. Dolbecq, L. Lisnard, A. Mallard, J. Marrot, F. Sécheresse, *Angew. Chem. Int. Ed.* **2002**, *41*, 2398-2401; c) J. N. Barrows, G. B. Jameson, M. T. Pope, *J. Am. Chem. Soc.* **1985**, *107*, 1771-1773; d) J. C. A. Boeyens, G. J. McDougal, J. Van R. Smit, *J. Solid State Chem.* **1976**, *18*, 191-199.

[10] a) X. López, J. M. Maestre, C. Bo, J.-M. Poblet, *J. Am. Chem. Soc.* **2001**, *123*, 9571-9576; b) T. Ueda, K. Kodani, H. Ota, M. Shiro, S.-X. Guo, J. F. Boas, A. M. Bond, *Inorg. Chem.* **2017**, *56*, 3990-4001.

[11] a) Y. Kikukawa, K. Yamaguchi, N. Mizuno, *Inorg. Chem.* **2010**, *49*, 8194-8196; b) D. Zhang, Z. Liang, S. Liu, L. Li, P. Ma, S. Zhao, H. Wang, J. Wang, J. Niu, *Inorg. Chem.* **2017**, *56*, 5537-5543; c) R. S. Winter, J. M. Cameron, L. Cronin, *J. Am. Chem. Soc.* **2014**, *136*, 12753-12761; d) J. Gao, J. Yan, S. Beeg, D.-L. Long, L. Cronin, *Angew. Chem. Int. Ed.* **2012**, *51*, 3373-3376; e) D.-L. Long, P. Kögerler, A. D. C. Parenty, J. Fielden, L. Cronin, *Angew. Chem. Int. Ed.* **2006**, *45*, 4798-4803; f) G. E. Sigmon, D. K. Unruh, J. Ling, B. Weaver, M. Ward, L. Pressprich, A. Simonetti, P. C. Burns, *Angew. Chem. Int. Ed.* **2009**, *48*, 2737-2740; g) D. K. Unruh, A. Burtner, L. Pressprich, G. E. Sigmon, P. C. Burns, *Dalton Trans* **2010**, *39*, 5807-5813.

[12] a) A. Müller, P. Gouzerh, *Chem. Soc. Rev.* **2012**, *41*, 7431-7463; b) R.-D. Lai, J. Zhang, X.-X. Li, S.-T. Zheng, G.-Y. Yang, *J. Am. Chem. Soc.* **2022**, *144*, 19603-19610. c) S. Kopilevich, A. Müller, I. A. Weinstock, *J. Am. Chem. Soc.* **2015**, *137*, 12740-12743; d) W.-J. Liu, G. Yu, M. Zhang, R.-H. Li, L.-Z. Dong, H.-S. Zhao, Y.-J. Chen, Z.-F. Xin, S.-L. Li, Y.-Q. Lan, *Small Methods* **2018**, *2*, 1800154; e) T. Liu, M. L. K. Langston, D. Li, J. M. Pigga, C. Pichon, A. M. Todea, A. Müller, *Science* **2011**, *331*, 1590-1592.

[13] a) W. Xuan, A. J. Surman, H. N. Miras, D.-L. Long, L. Cronin, *J. Am. Chem. Soc.* **2014**, *136*, 14114-14120; b) A. Müller, J. Meyer, E. Krickemeyer, E. Diemann, *Angew. Chem. Int. Ed.* **1996**, *35*, 1206-1208.

[14] A. Müller, E. Krickemeyer, H. Bögge, M. Schmidtmann, F. Peters, *Angew. Chem. Int. Ed.* **1998**, *37*, 3359-3363.

[15] a) J. Lin, N. Li, S. Yang, M. Jia, J. Liu, X.-M. Li, L. An, Q. Tian, L.-Z. Dong, Y.-Q. Lan, *J. Am. Chem. Soc.* **2020**, *142*, 13982-13988. b) E. Garrido. Ribó, N. L. Bell, W. Xuan, J. Luo, D.-L. Long, T. Liu, L. Cronin, *J. Am. Chem. Soc.* **2020**, *142*, 17508-17514. c) E. Garrido. Ribó, N. L. Bell, D.-L. Long, L. Cronin, *Angew. Chem. Int. Ed.* **2022**, *61*, e202201672.

[16] Crystallographic data for ***L*-Mo$_{132}$**: monoclinic, *C2/m*, a=40.487(8) Å, *b*=29.672(5) Å, *c*=27.400(5) Å, *α*=90°, *β*=125.782(5)°, *γ*=90°, *V*=26703(9) Å^3, *Z*=2, R_1 (all data)=0.1041, wR_2 (all data)=0.2618, GOF=1.041. The crystallographic data has been delivered to Cambridge Crystallographic Data Centre with CCDC No. of 2235287. These data can be obtained from the CCDC via www.ccdc.cam.ac.uk/data_request/cif.

[17] L. Deng, X. Dong, D.-L. An, W.-Z. Weng, Z.-H. Zhou, *Inorg. Chem.* **2020**, *59*, 4874-4881.

[18] E. Garrido Ribó, N. L. Bell, W. Xuan, J. Luo, D.-L. Long, T. Liu, L. Cronin, *J. Am. Chem. Soc.* **2020**, *142*, 17508-17514.

[19] A. Müller, A. M. Todea, J. van Slageren, M. Dressel, H. Bögge, M. Schmidtmann, M. Luban, L. Engelhardt, M. Rusu, *Angew. Chem. Int. Ed.* **2005**, *44*, 3857-3861.

[20] Y. Zhang, H. Gan, C. Qin, X. Wang, Z. Su, M. J. Zaworotko, *J. Am. Chem. Soc.* **2018**, *140*, 17365-17368.

[21] a) H. He, X. Li, D. Huang, J. Luan, S. Liu, W. K. Pang, D. Sun, Y. Tang, W. Zhou, L. He, C. Zhang, H. Wang, Z. Guo, *ACS Nano* **2021**, *15*, 8896-8906. b) S. Fei, Y. Wang, H. Wu, N. Zheng, X. Fang and D. Liu, *ACS Appl. Energy Mater.* **2022**, *5*, 10562–10571.

[22] a) K. d. A. Dias, M. V. P. Pereira Junior, L. H. Andrade, *Green Chem.* **2021**, *23*, 2308-2316; b) V. Y. Evtushok, A. N. Suboch, O. Y. Podyacheva, O. A. Stonkus, V. I. Zaikovskii, Y. A. Chesalov, L. S. Kibis, O. A. Kholdeeva, *ACS Catal.* **2018**, *8*, 1297-1307.

[23] a) S. Chang, Y. Chen, H. An, Q. Zhu, H. Luo, Y. Huang, *Green Chem.* **2021**, *23*, 8591-8603; b) C. W. Anson, S. Ghosh, S. Hammes-Schiffer, S. S. Stahl, *J. Am. Chem. Soc.* **2016**, *138*, 4186-4193.

10.1002/anie.202304728

WILEY-VCH

RESEARCH ARTICLE

Entry for the Table of Contents

A new structural variant (***L*-Mo132**) of the giant Keplerate type polyoxometalate Mo_{132} (***K*-Mo_{132}**) was synthesized. It which features lantern type structure and contains multiple terminal coordinated H_2O molecules on the outer surface. Its catalytic activity for the phenol oxidation reaction is superior to that of ***K*-Mo_{132}**.